Chin. J. Mech. Eng. (2017) 30:866–875
DOI 10.1007/s10033-017-0105-5

ORIGINAL ARTICLE

Optimum Tilt Angle of Flow Guide in Steam Turbine Exhaust Hood Considering the Effect of Last Stage Flow Field

Lihua CAO[1] · Aqiang LIN[1] · Yong LI[1] · Bin XIAO[1]

Received: 7 January 2016 / Revised: 20 June 2016 / Accepted: 26 August 2016 / Published online: 18 March 2017

Abstract Heat transfer and vacuum in condenser are influenced by the aerodynamic performance of steam turbine exhaust hood. The current research on exhaust hood is mainly focused on analyzing flow loss and optimal design of its structure without consideration of the wet steam condensing flow and the exhaust hood coupled with the front and rear parts. To better understand the aerodynamic performance influenced by the tilt angle of flow guide inside a diffuser, taking a 600 MW steam turbine as an example, a numerical simulator CFX is adopted to solve compressible three-dimensional (3D) Reynolds time-averaged N-S equations and standard k-ε turbulence model. And the exhaust hood flow field influenced by different tilt angles of flow guide is investigated with consideration of the wet steam condensing flow and the exhaust hood coupled with the last stage blades and the condenser throat. The result shows that the total pressure loss coefficient and the static pressure recovery coefficient of exhaust hood change regularly and monotonously with the gradual increase of tilt angle of flow guide. When the tilt angle of flow guide is within the range of 30° to 40°, the static pressure recovery coefficient is in the range of 15.27% to 17.03% and the total pressure loss coefficient drops to approximately 51%, the aerodynamic performance of exhaust hood is significantly improved. And the effective enthalpy drop in steam turbine increases by 0.228% to 0.274%. It is feasible to obtain a reasonable title angle of flow guide by the method of coupling the last stage and the condenser throat to exhaust hood in combination of the wet steam model, which provides a practical guidance to flow guide transformation and optimal design in exhaust hood.

Keywords Steam turbine · Exhaust hood · Last stage blades · Tilt angle of flow guide · Aerodynamic performance

1 Introduction

Exhaust hood connected with the last stage blades and the condenser throat is a main part of steam turbine which guides exhaust steam and improves the aerodynamic performance. The diffuser in the exhaust hood which consists of a guiding cone and a flow guide can accelerate the conversion of the leaving-velocity kinetic energy of exhaust steam into pressure energy because of the expansion effect on its passage section and accomplishes the process of static pressure recovery in exhaust hood. Therefore, the diffuser is the main factor affecting the aerodynamic performance of exhaust hood. The aerodynamic performance can be improved through the structure optimization design of the diffuser [1].

For many years, research on flow in steam turbine exhaust hood is mainly by scale-model experiment approach and numerical simulation. In general, the real flow in exhaust hood cannot be fully reflected by the scale-model experiment while a more detailed flow field data can be obtained by numerical simulation which is widely used in many fields, such as the optimal design of centrifugal compressor or turbine stage [2, 3]. By comparatively study

Supported by National Natural Science Foundation of China (Grant Nos. 51576036, 51476192), and Science and Technology Development Planning Foundation of Jilin Province of China (Grant No. 20140204040SF).

✉ Lihua CAO
clh320@163.com

[1] School of Energy and Power Engineering, Northeast Dianli University, Jilin 132012, China

the results of scale-model experiment and numerical simulation for exhaust hood, it is found that numerical simulation results are more accurate and reliable [4, 5]. To thoroughly understand the influence mechanism of the diffuser on the aerodynamic performance of the exhaust hood flow field, different methods are used to analyze the optimal design of the diffuser. CAO, et al [6], numerically simulated the real flow condition in exhaust hood at different inlet wetness, angle, and swirl strength. They found that the static pressure recovery coefficient and the total pressure loss coefficient of exhaust hood regularly changed at different inlet conditions. Furthermore, the results of the numerical simulation using 3D computational fluid dynamics (CFD) needed to be validated. ZHANG, et al [7], ZHOU, et al [8], and LIU, et al [9], comparatively studied the results of scale-model experiment and numerical simulation for exhaust hood computational model coupled with the last stage. The results showed the static pressure recovery of exhaust hood achieved mainly by the diffuser, and the swirl flow in exhaust hood was a main factor in decreasing the ability of static pressure recovery. BURTON, et al [10], and KREITMEIER, et al [11], summarized the research on the effects of diffuser structure on the aerodynamic performance of steam turbine exhaust hood. They emphasized that the main factors affecting the diffuser performance were the swirl flow of the last stage and the blade tip leakage flow. In order to study the performance of the diffuser, the methods of numerical calculation and optimal design to modify diffuser in exhaust hood were adopted by MIZUMI and ISHIBASHI [12]. Their research showed that the diffuser was an important component affecting the ability of static pressure recovery in exhaust hood. By parameterization of the diffuser in exhaust hood, VERSTRAETE, et al 13], WANG, et al [14], and CHEN, et al [15], used numerical simulation to analyze the aerodynamic performance of the exhaust hood after optimization. YOON, et al [16], MUSCH, et al [17], and BURTON, et al [18], proposed a steam separation zone near the flow guide that depended on the flow guide structure and the blade tip leakage flow of the last stage. In addition, they found that the steam separation was suppressed and the static pressure recovery was improved by the optimal design of flow guide structure. KREITMEIER, et al [11], and FAN, et al [19], showed that the reasonable tilt angle of flow guide could reduce the flow separation inside the diffuser. Although the static pressure recovery of the diffuser was promoted by the tilt angle, the researchers didn't provide the tilt angle range for the flow guide to improve the aerodynamic performance of the diffuser.

The results above show that one of the most important factors in deciding the aerodynamic performance of the diffuser is the last stage flow field. Therefore, the present study aims to determine the influence of flow guide tilt angle on the exhaust hood flow field in the diffuser. CFX 14.0 computational software platform is used to numerically simulate the flow field of exhaust hood considering the effect of the last stage flow field in a 600 MW steam turbine made in China. The aerodynamic performance generated by six different tilt angles of flow guide is discussed in detail, and the performance indices of exhaust hood are evaluated quantitatively to obtain a reasonable tilt angle range α of flow guide. In addition, the wet steam condensing flow and the condenser throat flow field are considered in the process of numerical simulation. The research results of the paper offer a reference for the optimization design and performance study of the diffuser.

2 Numerical Simulation Method

2.1 Computational Model and Mesh

The structure diagram of the typical low pressure (LP) exhaust hood in a 600 MW supercritical steam turbine is shown in Fig. 1. The last stage exhaust steam firstly flows through the diffuser consisting of a flow guide and a guiding cone. The diffuser has a guiding flow function, thus, the flow is turned to 90° from the axial direction to the radial direction. Then the exhaust steam flows in the downstream condenser through the condenser throat. Both the exhaust hood and the condenser throat constitute the LP exhaust passage. Therefore, the computational domain in this study mainly considers the last stage blades, LP exhaust hood, condenser throat, and LP heater. The simplified schematic diagram of exhaust hood is shown in Fig. 2, and the 3D computational model for the exhaust passage is shown in Fig. 3. The geometric parameters of the exhaust passage in the calculated domain are provided in Table 1. Clockwise along the z axis

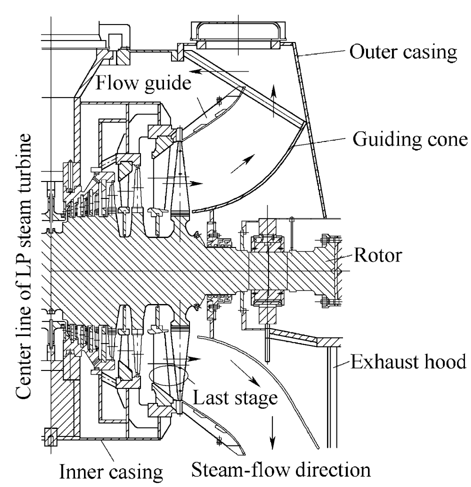

Fig. 1 Schematic diagram of the typical LP exhaust hood in a 600 MW steam turbine

of the Cartesian coordinate system, curves (1, 2, 3, and 4) are selected from the flow guide wall for the back analysis, as shown in Fig. 2.

Using ICEM CFD 14.0 software, the computational domain in the exhaust passage is divided into unstructured tetrahedral mesh. A total of 52 pieces of stator blade and 80 pieces of rotor blade are divided into structured mesh by TurboGrid 14.0 software, as shown in Fig. 4. The HOH-type grids are used for the stator and rotor blades domain. By contrast, the orthogonal H-type grids are utilized for the blade inlet domain, blade outlet domain and blade tip clearance. The meshes are compressed next to the solid wall so as to achieve y^+ value of 1 at the rotor domain and of 5 at the stator domain. To ensure the calculation accuracy, a study of grid independence is conducted, and it shows that the grid numbers in computational domain for the exhaust passage, stator blade, and rotor blade of the last stage are approximately 2.5 million, 2.7 million, and 4 million, respectively.

2.2 Numerical Method

Using the commercial CFD simulator CFX 14.0, the 3D compressible steady-state Reynolds time-averaged N-S equations are solved by finite volume method. A solution method of SIMPLE algorithm based on pressure-velocity coupling is used. The standard k-ε turbulence model combining with the scalable wall function is adopted. For the advection term, a high resolution scheme is applied to spatial discrete. The equations are converged when the residual absolute criteria value is less than 1e-5 in the present analysis. The interfaces, including that between the stator cascade and rotor cascade and that between the rotor cascade and exhaust hood, adopt frozen-rotor model. The working fluid is wet steam selected steam3vl model in the IAPWS-IF97 library, which can reflect the wet steam two-phase condensing flow. The steam parameters are taken from the steam turbine heat acceptance (THA) operation condition. The inlet mass flow rate, total temperature, and

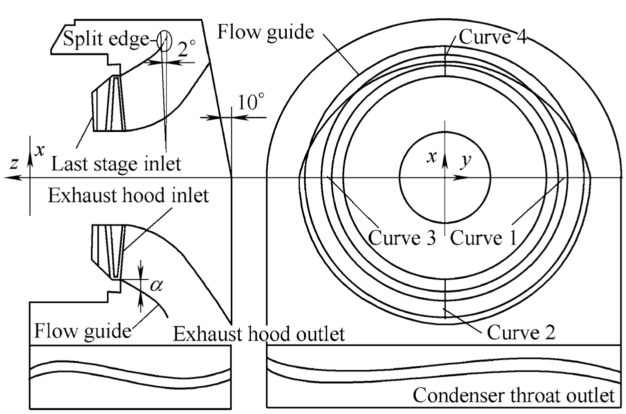

Fig. 2 Simplified model of exhaust hood

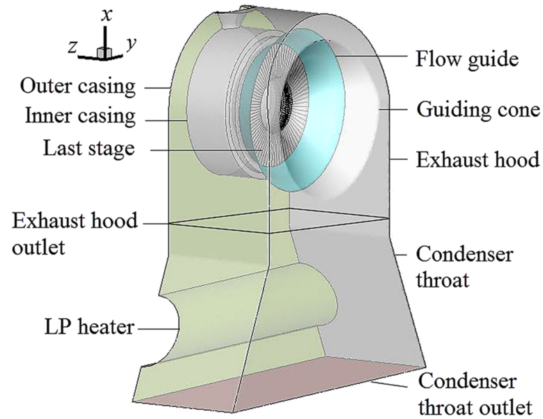

Fig. 3 Computational model of exhaust passage

Table 1 Geometry structure of computational domain

Domain	Geometric structure parameters	
Last stage blade	Tip clearance δ/m	0.011 2
	Rotor-blade height H_1/m	1.029
Exhaust hood	Height H_2/m	6.065
	Area of outlet section A_1/m^2	3.740×6.580
Condenser throat	Height H_3/m	5.580
	Radius of heater D/m	1.040
	Area of outlet section A_2/m^2	3.740×10.550

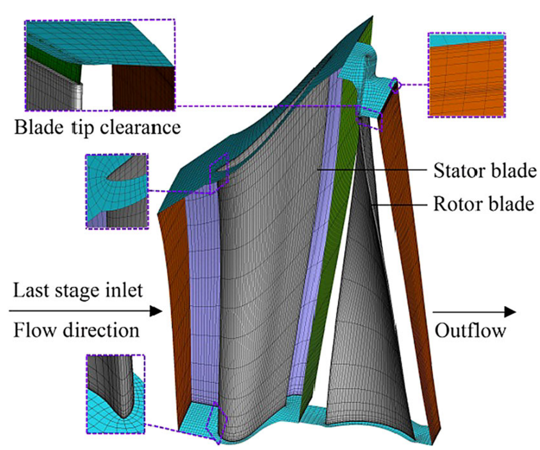

Fig. 4 Computational mesh of a last stage blades passage

steam wetness are set at 67.783 kg/s, 335.05 K, and 0.055, respectively, for the inlet of the last stage, which is the boundary condition of mass flow inlet. The average static pressure at the condenser throat outlet, which is the pressure-outlet boundary condition, is fixed at 4900 Pa.

To evaluate quantitatively the aerodynamic performance of the LP exhaust passage flow field at different tilt angles of flow guide, the parameter values of average velocity and pressure are adopted for the calculation [20]. The averaging process is described as follows:

$$p = \frac{\int p_i \rho_i v_i \mathrm{d}A}{\int \rho_i v_i \mathrm{d}A}, V_{\mathrm{m}} = \frac{\int v_i \rho_i \mathrm{d}A}{\int v_i \mathrm{d}A}, V_{\mathrm{a}} = \frac{\int v_i \mathrm{d}A}{\int \mathrm{d}A}, \tag{1}$$

where p and V_{m} represent respectively the mass-weighted average pressure and velocity, V_{a} is the area-weighted average velocity, p_i, ρ_i and v_i represent respectively the i-th elemental area of pressure, density, and velocity, and dA is the local incremental area.

3 Results and Discussion

3.1 Flow Field Analysis—Exhaust Passage

The diffuser located at the inlet section of exhaust hood acts as the role of guiding flow, increasing pressure and decreasing flow loss. The aerodynamic performance in exhaust passage is directly influenced by the diffuser structure and the flow condition of exhaust hood inlet. The flow loss in exhaust passage changes with different tilt angles of flow guide. Therefore, the following is a detailed analysis of the exhaust passage flow field at 35° tilt angle.

The velocity vector diagram is presented in Fig. 5, which shows that the inlet velocity vector of exhaust hood is affected by the last stage and the blade tip clearance.

As shown in Fig. 5, the velocity magnitude at the exhaust hood inlet is not evenly distributed, whereas the middle-low part of the rotor blade clearly presents a higher velocity vector. A small amount of the exhaust steam forms a leakage flow as flowing through the blade tip clearance because it remains in the velocity tangential component at the stator blade outlet. Most of the exhaust steam expands through the rotor blade to do work and the outlet steam angle changes. The direction of velocity vector of leakage flow is opposite with that of the rotor blade outlet. So, the exhaust steam flow into the diffuser at different speeds.

For a more intuitive display of steam velocity distribution at the exhaust hood inlet, the circumference of 90°, 0°, –90°, and 180° along the blade height are used to select four auxiliary lines. The velocity distribution of the corresponding location is presented in Fig. 6.

Fig. 6 shows that the difference of velocity along the circumferential distribution of four lines is small, and the velocity at the rotor blade outlet is within the range of 100 m/s to 200 m/s. The velocity rises gently along the blade height direction from the hub to 45% blade height, whereas the velocity gradually reduces from the maximum to the minimum value on the blade height within the range of 45% to 80%. Then, the velocity shows a dramatic increase from 80% blade height to the tip. The velocity of the last stage outlet along the blade height presents the "v" type of change because of the gravity and the centrifugal force of the blade resulting in the large mass flow in the lower part of the blade. At 45% blade height, the steam separates centrifugally and flows to the blade tip. The result shows a rapid increase of mass flow from 80% blade height to the tip. This phenomenon is caused by two reasons. Firstly, it is the result of flow design which has various cross-sections at the last twisted blade. Secondly, it is affected by mass flow distribution caused by high speed rotation of the blade. The velocity of the blade tip leakage distribution is within the range of 165 m/s to 190 m/s. Due to the small blade tip clearance, this portion of the mass flow goes directly into the exhaust hood in the form of jet flow.

The 3D velocity streamline at a certain moment in the exhaust passage is shown in Fig. 7. Evidently, the steam presents a complex 3D swirl flow in the exhaust passage. With the direction of steam changes from axial to radial direction, it first flows through the diffuser, and then flows

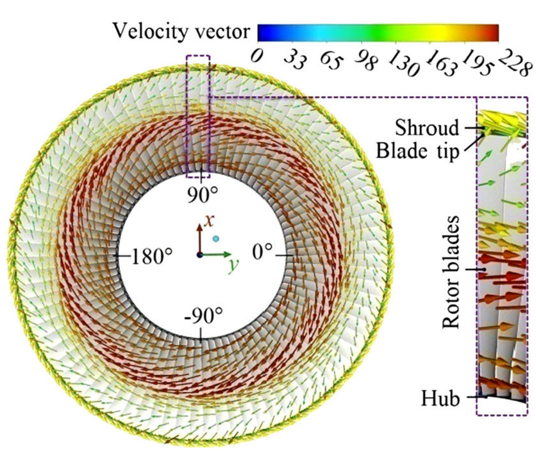

Fig. 5 Velocity vector at exhaust hood inlet section (m • s^{-1})

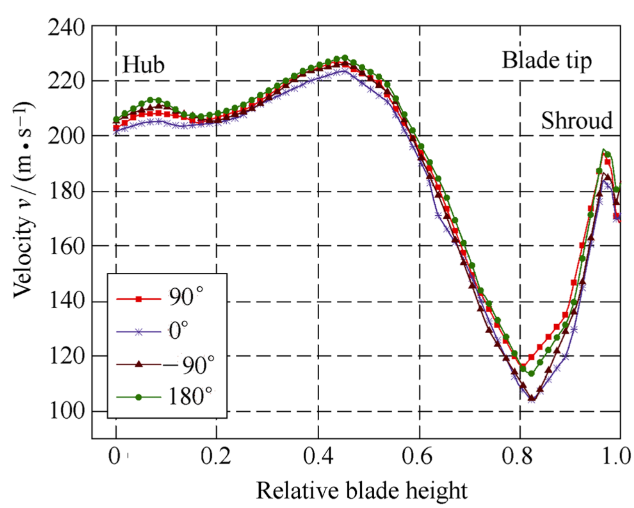

Fig. 6 Velocity curve along each blade height direction

into downstream passage. A portion of steam directly impinges the wall making the velocity high. And, another portion of the steam changes the direction at the axial and radial velocity component because the steam swirls and collides with each other, thereby resulting in high flow loss and low-velocity vortex. When the steam flows along the upper half of the diffuser to the top region in exhaust hood, it easily forms vortex because the exhaust hood on the top is closed and the space is narrow, as shown in detail in Fig. 8. The vortex on the top of the exhaust hood flows respectively along the positive and negative directions of the y axial to downstream and forms two obvious vortices (Vortex 1 and Vortex 2) at the horizontal middle plane of exhaust hood. The two vortices induce mutually convection in the downstream passage, which affect the flow loss, the aerodynamic performance of exhaust passage and the flow field of the condenser throat outlet. The rollover effect of steam at the top of exhaust hood changes with the change of the tilt angle. Therefore, the aerodynamic performance in the exhaust passage can be improved.

Fig. 9 shows the result of static pressure distribution at the flow guide intra-wall. The pressure is the lowest at the entrance section of the diffuser and then gradually increases with the steam flowing in flow guide which plays the role of the static pressure recovery. As steam flows through the diffuser along the axial direction, a noticeable flow separation or flow loss close to the flow guide wall does not occur because of the blade tip leakage flow, which results in a low static pressure value. To a certain extent, the blade tip leakage flow improves the aerodynamic performance of the diffuser. Fig. 9 shows that the static pressure value in the lower half of the flow guide is uniformly distributed, whereas the static pressure value in the upper half is high in a large area because the flow velocity decreases and the static pressure increases with the steam in the diffuser flowing from the axial to the radial direction. At the same time, the steam in the lower half of the diffuser directly flows into the downstream passage, and it has a low resistance to flow. However, the steam in the upper half of the diffuser has insufficient space to achieve pressure increase because the top of exhaust hood flow space becomes smaller. Meanwhile, the steam collides with each other or with the wall, resulting in the increase of flow resistance. As a result, the upper half of the flow guide wall appears high pressure value. When the tilt angle of flow guide is changed, the velocity decrease and pressure increase in the diffuser can also be achieved.

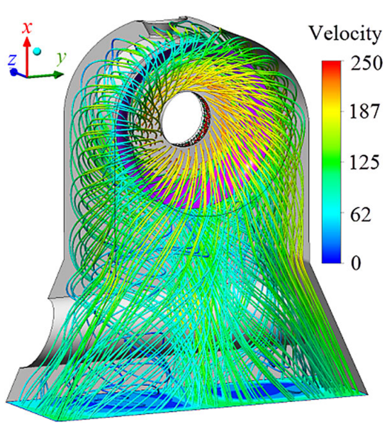

Fig. 7 3D streamlines ($m \cdot s^{-1}$)

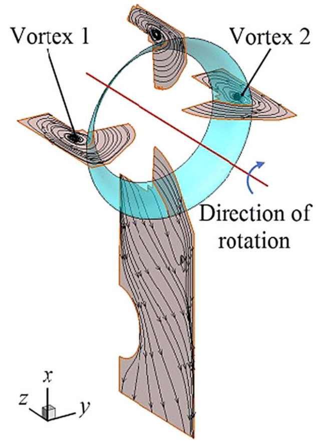

Fig. 8 2D streamlines

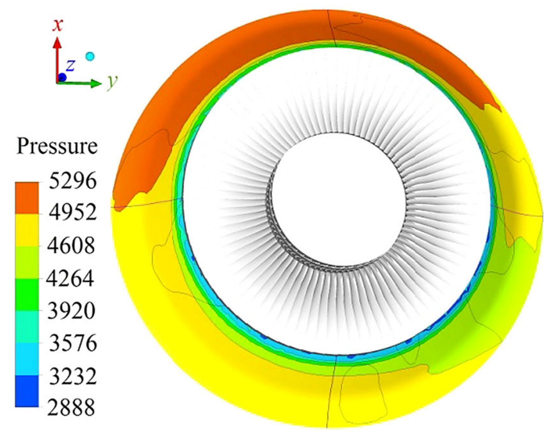

Fig. 9 Static pressure contours at the wall of flow guide (Pa)

The outlet velocity distribution at the exhaust hood and the condenser throat is presented in Fig. 10(a) and Fig. 10(b). The high velocity region appears near the wall and two major low velocity regions appear in the middle section because of the swirl flow of the upstream steam. The low velocity zone of the condenser throat outlet is larger than that of the exhaust hood outlet. The highest value of velocity decreases from 160 m/s at the exhaust hood outlet to 120 m/s at the throat outlet, which indicates that the kinetic energy of the two swirling is converted into pressure energy with the flow downstream.

The aerodynamic performance of exhaust hood directly affects the uniformity distribution of the downstream flow field. Therefore, velocity uniformity distribution can further reflect the impact caused by the two vortices. Table 2 shows that the uniformity coefficient of the velocity field is reduced from 74.003% to 65.896% with the steam flows downstream from the exhaust hood outlet to the condenser throat outlet. Through improving the flow field distribution of low velocity zone and the high velocity zone, the velocity distribution can be more uniform, which directly affects the security of condenser.

3.2 Flow Field Analysis—Tilt Angle of Flow Guide

Under the condition of the flow guide length unchanged, the flow space in the diffuser changes with the change of tilt angle of the flow guide, which causes different abilities of static pressure recovery. To better analyze the impact of the tilt angle on the aerodynamic performance, the exhaust passage is numerically simulated at tilt angles of 15°, 20°, 25°, 30°, 35°, and 40°.

A typical static pressure distribution contour on the meridian plane is shown in Fig. 11 at different tilt angles. As shown in Fig. 11, the static pressure obviously increases at the last stage outlet along the flow direction. And the static pressure rapidly declines to the range of 4 800 Pa to 5 200 Pa at the top of exhaust hood, which is close to 4 900 Pa given to a value at the condenser throat outlet. But the static pressure increases in the lower part of exhaust hood.

A comparison of Fig. 11 shows that with the increase of α, the static pressure value increases in the range of 5 100 Pa to 6 200 Pa and the pressure distribution in the diffuser becomes uniform. The effect scope of the vortex at the top of exhaust hood becomes small. The process of velocity decrease and the pressure increase in the diffuser can be improved with the change of the tilt angle of flow guide.

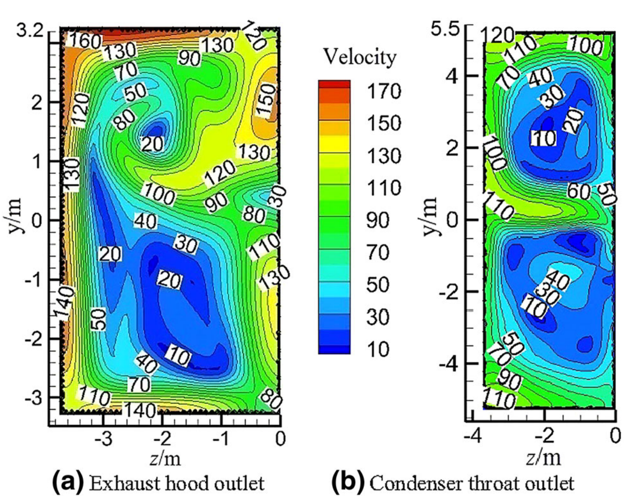

Fig. 10 Velocity distribution map at each outlet section (m • s^{-1})

The static pressure recovery ability and the aerodynamic performance in the diffuser are reflected by the static pressure distribution on inner sidewall of the flow guide. Fig. 12 shows the static pressure distribution on the inner sidewall of flow guide along the defined curves (Curves 1 to 4). With the steam flowing in the diffuser, the static pressure recovery degree is different at the four curves along the flow guide circumferential distribution. Therefore, the diffuser is the transition stage of the steam flowing into the LP exhaust passage. In addition, the steam in the diffuser has different degree inflation to make different static pressure distributions on the flow guide wall. A comparison of Fig. 12 shows that the static pressure values at the end of Curves 1 to 4 are higher than those in the beginning, which means that the diffuser plays a role of static pressure recovery. With an increase in the tilt angle of flow guide, the static pressure value at the beginning of curves gradually reduces, and the static pressure value drops under 4 100 Pa at α= 30°, 35°, and 40°, reaching to a lower exhaust pressure at the last stage outlet relative to that at α=15°, 20° and 25°. Along the flow direction, the static pressure values gradually increase to a peak at the beginning of curves to 20% normalized length because the velocity of steam decreases and the specific volume increases at the initial segment of the diffuser. Moreover, the flow guide restricts the radial expansion of the steam. At 20% length to the end of the curves, the static pressure slowly decreases and tends to be stable because the flow guide plays a transitional role with the steam turning from the axial direction to the radial direction. Therefore, the degree of static pressure recovery in the diffuser is small, which reduces flow loss of the steam in that region to a certain extent. As a result, a reasonable tilt angle of flow guide can achieve a better conversion of the leaving-velocity kinetic energy into pressure energy.

To quantitatively evaluate the impact of the tilt angle change on aerodynamic performance of the exhaust passage and to determine a reasonable range of the tilt angle, three indices for performance evaluation are introduced, namely, the velocity uniformity coefficient of condenser throat outlet (λ), the total pressure loss coefficient of exhaust hood (C_T), and the static pressure recovery coefficient of exhaust hood (C_S). Additionally, the lager λ value is, the more uniform the outlet velocity distributes. The smaller C_T value is, the smaller flow pressure loss is. The higher C_S value is, the more leaving-velocity kinetic energy convert into pressure energy in exhaust hood.

Table 2 Uniformity coefficient of outlet velocity field

Computational results	Exhaust hood outlet	Condenser throat outlet
Mass-weighted velocity $V_a/(\mathrm{m} \bullet \mathrm{s}^{-1})$	83.441	55.355
Area-weighted velocity $V_m/(\mathrm{m} \bullet \mathrm{s}^{-1})$	112.753	84.003
Uniformity coefficient $\lambda/\%$	74.003	65.896

Three indices are defined as follows:

$$\lambda = \left(1 - \frac{|V_{\mathrm{m,out}} - V_{\mathrm{a,out}}|}{V_{\mathrm{m,out}}}\right) \times 100\% = \frac{V_{\mathrm{a,out}}}{V_{\mathrm{m,out}}} \times 100\%, \quad (2)$$

$$C_{\mathrm{T}} = (p_{\mathrm{T,inlet}} - p_{\mathrm{T,outlet}})/(p_{\mathrm{T,inlet}} - p_{\mathrm{S,inlet}}), \quad (3)$$

$$C_{\mathrm{S}} = (p_{\mathrm{S,outlet}} - p_{\mathrm{S,inlet}})/(p_{\mathrm{T,inlet}} - p_{\mathrm{S,inlet}}), \quad (4)$$

where $V_{\mathrm{m,out}}$ and $V_{\mathrm{a,out}}$ represent respectively the mass-weighted average velocity and area-weighted average velocity at condenser throat outlet, $p_{\mathrm{S,inlet}}$ and $p_{\mathrm{T,inlet}}$ represent respectively the static pressure and total pressure at exhaust hood inlet, $p_{\mathrm{S,outlet}}$ and $p_{\mathrm{T,outlet}}$ are the static pressure and total pressure at exhaust hood outlet, respectively.

Fig. 13 and Fig. 14 show the change of the performance evaluation indices of exhaust hood at different tilt angles of flow guide. Fig. 13 shows that λ have no obvious change with increasing of the tilt angles, illustrating the minimal effect of the tilt angle on the velocity field at the condenser throat outlet. On the contrary, the C_{T} decreases from the peak value of 79.12% to a minimum value of 50.67%, appearing to be substantial fluctuations. When the tilt angle lies within the range of 15° to 35° and 35° to 40°, the C_{T} monotonically decreases and increases, respectively. When the tilt angle of flow guide is within the range of 30° to 40°, the total pressure loss of exhaust hood is relatively low.

Fig. 14 shows that with the increase of the tilt angle, the C_{S}have a trend of monotone increase to monotone decrease. Under the condition of α=15°−20°, $C_{\mathrm{S}}$is a negative value, suggesting that the exhaust hood does not play a role of recovering pressure but accelerates the flow loss. However, when α=20°−40°, $C_{\mathrm{S}}$is a positive value because the leaving-velocity kinetic energy is converted into pressure energy in exhaust hood. When α is 35°, C_{S}value is the peak of 0.17. According to Fig. 13 and Fig. 14, when the tilt angle of flow guide is less than 15° or more than 40°, it is predicted that the flow space between the flow guide and the guide cone increases or decreases, respectively, which slows down the aerodynamic performance of exhaust hood. As a result, the static pressure recovery ability of exhaust hood can be improved with reasonable tilt angles of flow guide.

Therefore, there is an optimum tilt angle at 30° to 40° range which will improve the aerodynamic performance of

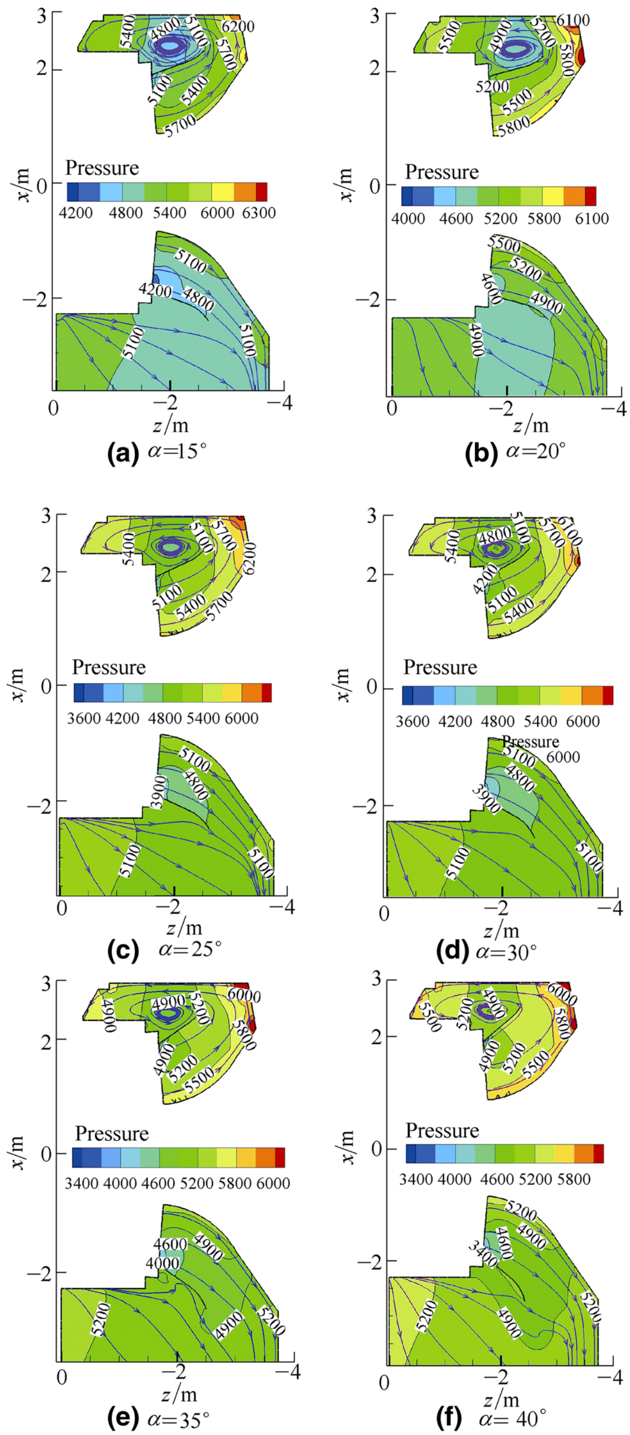

Fig. 11 Static pressure contours on meridian plane of exhaust hood at different tilt angles (Pa)

the diffuser and reduce the pressure loss generated by steam of the last stage outlet. Moreover, the static pressure recovery coefficient of exhaust hood is relatively high. It has a guiding significance to the optimized design of the diffuser and its performance study.

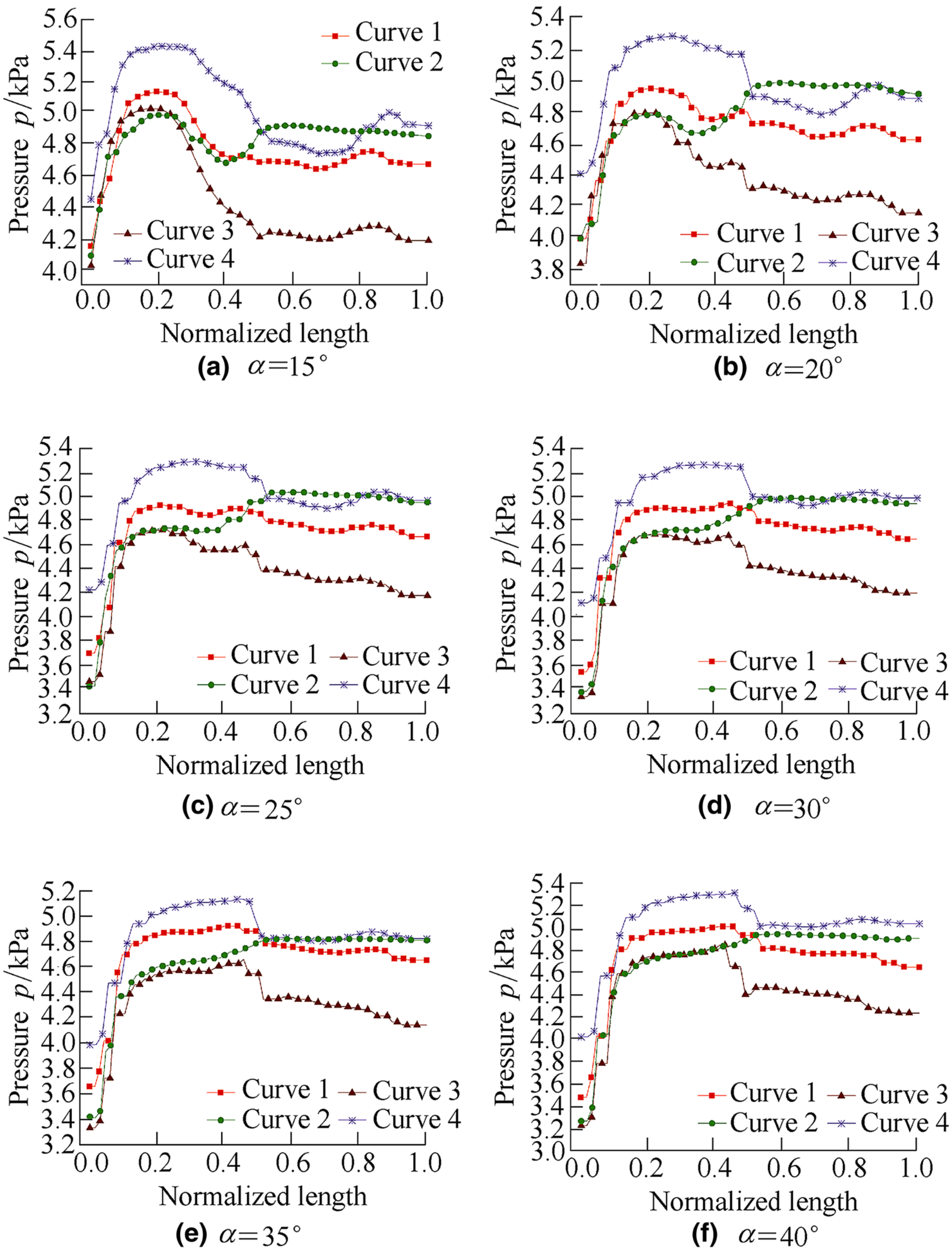

Fig. 12 Static pressure variations on inner sidewall axial direction curves of flow guide

3.3 Validation

To evaluate indices C_T and C_S, and to confirm the reliability of the tilt angle range of flow guide, the effective enthalpy drop that reflects an economy of steam turbine is introduced to verify the indices [21]. According to the proposal by SHEN [22], if 15.6 kJ/kg of the leaving-velocity kinetic energy of the last stage is used to increase the static pressure for the 600 MW steam turbine, the effective enthalpy drop increases by about 1%, which is expressed as

$$\Delta h = \left(\frac{1}{2}V_{\mathrm{m,inlet}}^2 - \frac{1}{2}V_{\mathrm{m,out}}^2\right) \times 10^{-3}, \tag{5}$$

where Δh represents the kinetic energy loss in exhaust passage, $V_{\mathrm{m,inlet}}$ is the mass-weighted average velocity at exhaust hood inlet.

The kinetic energy loss is converted into pressure drop, which can be written as

$$\Delta p = \frac{1}{2}\rho_{\mathrm{inlet}}V_{\mathrm{m,inlet}}^2 - \frac{1}{2}\rho_{\mathrm{out}}V_{\mathrm{m,out}}^2, \tag{6}$$

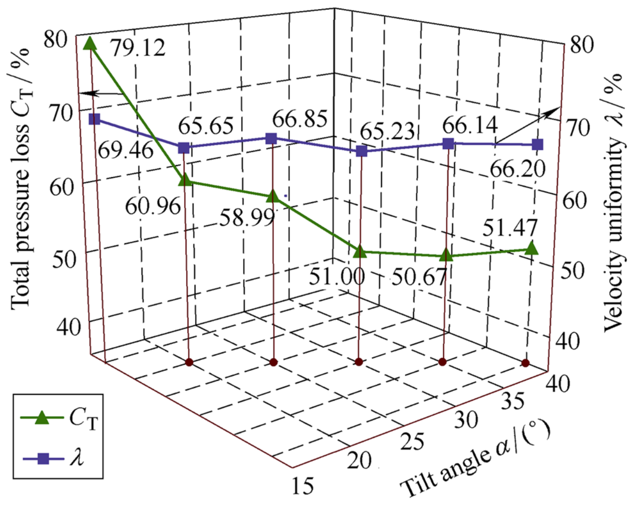

Fig. 13 Performance indices of exhaust hood

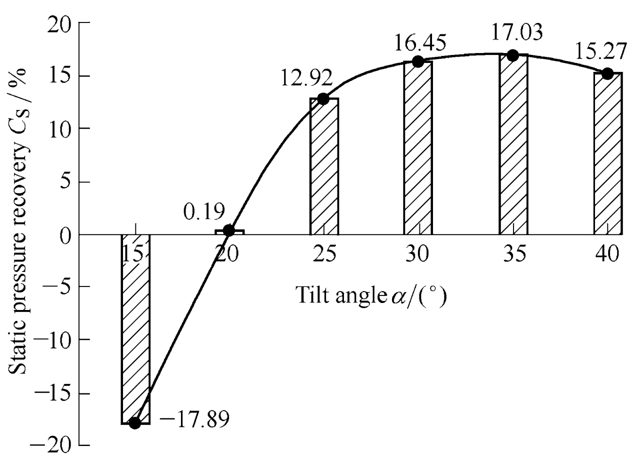

Fig. 14 Static pressure recovery coefficient of exhaust hood

where ρ_{inlet} and ρ_{out} are the weighted average density at exhaust hood inlet and at condenser throat outlet, respectively.

The increment of mass-weighted average static pressure in the exhaust passage is

$$\Delta p_S = p_{S,\text{out}} - p_{S,\text{inlet}}, \tag{7}$$

where $p_{S,\text{out}}$ is the static pressure at condenser throat outlet.

Then, the available kinetic energy h_r used for increasing the static pressure of exhaust hood can easily be computed by the following formula:

$$h_r = \frac{\Delta p_S}{\Delta p} \times \Delta h. \tag{8}$$

According to Eq. (8), $\Delta\eta$, which is the increment of the effective enthalpy drop can be defined as

$$\Delta\eta = (h_r/15.6) \times 1\%. \tag{9}$$

Fig. 15 shows the relation curve between the different tilt angles of flow guide and the effective enthalpy drop of steam turbine at THA operation condition. It can be seen from

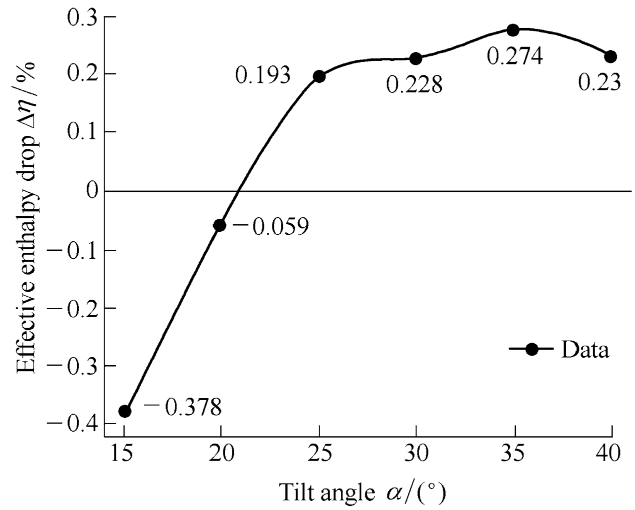

Fig. 15 Increment of steam turbine effective enthalpy drop at different tilt angles

Fig. 15 that the increment of the effective enthalpy drop presents a monotonically increasing trend (α is between 15° and 35°) and monotonically decreasing trend (α is between 35° and 40°). Moreover, when α is in the range of 15° to 20°, $\Delta\eta$ is a negative value caused by an unreasonable tilt angle of flow guide that reduces the economy of steam turbine. When α is at the 30° to 40° range, the value of $\Delta\eta$ is in the range of 0.228% to 0.274% which is higher than those of other tilt angle range. And this range of 30° to 40° is identical with the analysis of C_T and C_S respectively in Fig. 13 and Fig. 14. So it is reasonable and feasible that the evaluation indices of exhaust hood are used to determine the optimum tilt angle range for the best aerodynamic performance of the diffuser. Moreover, the flow guide can disassemble and assemble easily for transformation.

4 Conclusions

(1) The blade tip leakage flow has high velocity and its swirling direction is opposite to the steam direction of the last stage outlet, which has a significant impact on the aerodynamic performance of exhaust hood. The static pressure on the upper half wall of flow guide is higher than that on the lower half wall. The static pressure recovery on the upper half of the diffuser is better than that on the lower half.

(2) With the increase of the tilt angle, the total pressure loss coefficient has a decreasing-increasing tendency, and the static pressure recovery coefficient presents an increasing-decreasing tendency. However, the velocity uniformity coefficient changes slightly.

(3) When the tilt angle of flow guide is in the range of 30° to 40°, the static pressure recovery coefficient

and the total pressure loss coefficient of exhaust hood are within the range of 15.27% to 17.03% and 50.67% to 51.47%, respectively. Correspondingly, the increment of the effective enthalpy drop in steam turbine is within the range of 0.228% to 0.274%. Therefore, the optimum tilt angle lies in the range of 30° to 40° should be used for the structure design and the transformation of flow guide in a 600 MW steam turbine.

References

1. SAURET E, GU Y. Three-dimensional off-design numerical analysis of an organic rankine cycle radial-inflow turbine[J]. *Applied Energy*, 2014, 135: 202–211.
2. CHEN Zonghua, GU Chuangang, SHU Xinwei. Shape optimum design for centrifugal compressor radial inlet based on CFD technique[J]. *Journal of Mechanical Engineering*, 2010, 46(14): 124–129. (in Chinese).
3. ZHANG Hongtao, WANG Xiangfeng, YAN Peigang, et al. Simulation investigation on application of leaf seal in turbine stage[J]. *Journal of Mechanical Engineering*, 2014, 50(12): 177–184. (in Chinese).
4. VEERABATHRASWAMY K, SENTHIL KUMAR A. Effective boundary conditions and turbulence modeling for the analysis of steam turbine exhaust hood[J]. *Applied Thermal Engineering*, 2016, 103: 773–780.
5. RIS V V, SIMOYU L L, GALAEV A S, et al. Numerical simulation of flow in a steam turbine exhaust hood: comparison results of calculations and data from a full scale experiment[J]. *Thermal Engineering*, 2009, 56(4): 277–283.
6. CAO Lihua, LIU Jia, LI Yong, et al. 3D numerical analysis of wet steam flow in exhaust hoods of steam turbines[J]. *Proceedings of the CSEE*, 2012, 32(29): 79–86. (in Chinese).
7. ZHANG W, PAIK B G, JANG Y G, et al. Particle image velocimetry measurements of the three-dimensional flow in an exhaust hood model of a low-pressure steam turbine[J]. *Journal of Engineering for Gas Turbines and Power*, 2007, 129(2): 411–419.
8. FU J L, LIU J J, ZHOU S J. Experimental and numerical investigation of interaction between turbine stage and exhaust hood[J]. *Proceedings of the Institution of Mechanical Engineers, Part A: Journal of Power and Energy*, 2007, 221(7): 991–999.
9. LIU J J, CUI Y Q, JIANG H D. Investigation of flow in a steam turbine exhaust hood with/without turbine exit conditions simulated[J]. *Journal of Engineering for Gas Turbines and Power*, 2003, 125(1): 292–299.
10. BURTON Z, INGRAM G L, HOGG S. A literature review of low pressure steam turbine exhaust hood and diffuser studies[J]. *Journal of Engineering for Gas Turbines and Power*, 2013, 135(6): 062001-1–10.
11. KREITMEIER F, GREIM R. Optimization of blade-diffuser interaction for improved turbine performance[J]. *Proceedings of the Institution of Mechanical Engineers, Part A: Journal of Power and Energy*, 2003, 217(4): 443–451.
12. MIZUMI S, ISHIBASHI K. Design philosophy and methodology of a low pressure exhaust hood for a large power steam turbine[C]// *Proceedings of ASME Turbo Expo 2013: Turbine Technical Conference and Exposition*, San Antonio, USA, June 3–7, 2013: V05BT25A007.
13. VERSTRAETE T, PRINSIER J, SANTE A D, et al. Design optimization of a low pressure steam turbine radial diffuser using an evolutionary algorithm and 3D CFD[C]//*Proceedings of ASME Turbo Expo 2012: Turbine Technical Conference and Exposition*, Copenhagen, Denmark, June 11–15, 2012: 603–613.
14. WANG H T, ZHU X C, DU Z H. Aerodynamic optimization for low pressure turbine exhaust hood using kriging surrogate model[J]. *International Communications in Heat Mass Transfer*, 2010, 37(8): 998–1 003.
15. CHEN Chuan, Fu Jinglun, LIU Jianjun. Optimal design and performance analysis of steam turbine exhaust system[J]. *Journal of Engineering Thermophysics*, 2009, 30(8): 1 295–1 298. (in Chinese).
16. YOON S, STANISLAUS F J, MOKULYS T, et al. A three-dimensional diffuser design for the retrofit of a low pressure turbine using in-house exhaust design system[C]//*Proceedings of ASME Turbo Expo 2011: Turbine Technical Conference and Exposition*, Vancouver, Canada, June 6–10, 2011: 2 309–2 319.
17. MUSCH C, STÜER H, HERMLE G. Optimization strategy for a coupled design of the last stage and the successive diffuser in a low pressure steam turbine[J]. *Journal of Turbomachinery*, 2013, 135(1): 011013.
18. BURTON Z, INGRAM G L, HOGG S. The influence of condenser pressure variation and tip leakage on low pressure steam turbine exhaust hood flows[J]. *Proceedings of the Institution of Mechanical Engineers, Part A: Journal of Power and Energy*, 2014, 228(4): 370–379.
19. FAN T, XIE Y H, ZHANG D, et al. A combined numerical model and optimization for low pressure exhaust system in steam turbine[C]//*Proceedings of ASME Turbo Expo 2007: Turbine Technical Conference and Exposition*, San Antonio, USA, July 17–19, 2007: 349–358.
20. TINDELL R H, ALSTON T M, SARRO C A, et al. Computational fluid dynamics analysis of a steam power plant low-pressure turbine downward exhaust hood[J]. *Journal of Engineering for Gas Turbines and Power*, 1996, 118(1): 214–224.
21. YAZAWA K, KOH Y R, SHAKOURI A. Optimization of thermoelectric topping combined steam turbine cycles for energy economy[J]. *Applied Energy*, 2013, 109: 1–9.
22. SHEN Shiyi, ZHUANG Heqing, KANG Shong. *Principles of steam turbine*[M]. Beijing: China Electric Power Press, 1991. (in Chinese).

Lihua CAO born in 1973, is currently a professor at *School of Energy and Power Engineering, Northeast Dianli University, China*. Her research interests include economic analysis and optimization operation of steam turbine and its auxiliaries. Tel: +86-432-64806902; E-mail: clh320@163.com

Aqiang LIN born in 1988, is currently a master candidate at *School of Energy and Power Engineering, Northeast Dianli University, China*. His research interests are numerical simulation and optimum design on aerodynamic performance of exhaust system in steam turbine. E-mail: linaqiang493@sina.com

Yong LI born in 1964, is currently a professor and a PhD supervisor at *School of Energy and Power Engineering, Northeast Dianli University, China*. His research interests include performance testing and optimizing operation of steam turbine. Tel: +86-432-64806610; E-mail: liyong6883@163.com

Bin XIAO born in 1978, is currently a professor at *School of Energy and Power Engineering, Northeast Dianli University*, *China*. His research interests include vibration, noise control and signal processing. Tel: +86-432-64806772; E-mail: binxiao@yahoo.cn